Catalysis Today 175 (2011) 485–493

Contents lists available at ScienceDirect

Catalysis Today

journal homepage: www.elsevier.com/locate/cattod

Optimal synthesis of micro/mesoporous beta zeolite from kaolin clay and catalytic performance for hydrodesulfurization of diesel

Aijun Duan[a], Guofu Wan[b], Ying Zhang[c], Zhen Zhao[a,*], Guiyuan Jiang[a], Jian Liu[a]

[a] State Key Laboratory of Heavy Oil Processing, China University of Petroleum, Beijing 102249, China
[b] College of Mechanical and Energy Engineering, Jiangsu Polytechnic University, Changzhou 213164, China
[c] Department of Materials Science and Engineering, China University of Petroleum, Beijing 102249, China

ARTICLE INFO

Article history:
Received 26 October 2010
Received in revised form 16 February 2011
Accepted 16 March 2011
Available online 30 April 2011

Keywords:
Kaolin clay
Zeolite beta
In situ hydrothermal crystallization method
Supported catalysts
Hydrodesulfurization

ABSTRACT

To be used as the unique sources of silica and alumina, kaolin clay was pretreated by different kinds of acids including H_2SO_4, HCl and H_3PO_4. Through evaluating the synthesis factors of the kaolin clay pretreatment and the crystallization of beta zeolite systematically, the optimal conditions were obtained, i.e., using HCl concentrations of 8.2 mol/L to process kaolin clay at 96 °C for 3 h, and the optimal H_2O/SiO_2 of 3–4, $TEAOH/SiO_2$ ratio of 0.06, Na_2O/SiO_2 ratio of 0.05 for crystallizing at 170 °C more than 16 h. The typical physico-chemical properties of samples were characterized by the techniques of XRD, N_2-adsorption and FT-IR. The supported NiMo/Beta-Al_2O_3 series catalysts with different beta contents were prepared and evaluated in a fixed bed microreactor with FCC diesel. HDS results indicated that NiMo/Beta-Al_2O_3 series catalysts exhibited higher HDS activities compared with the conventional NiMo/Al_2O_3 catalysts, and S in the best product obtained over the catalyst with beta content of 32% was 8.4 $\mu g\,g^{-1}$ which met the S regulation of ultra clean diesel in Euro-V specification. Combined with the sulfur distributions by GC–PFPD method, it could be found that the incorporation of acidic zeolite in the support could favor the deep removal of sulfur compounds.

1. Introduction

Due to the increasing attention on the environmental protection, highly stringent demands of environmental legislation impel the specifications of ultra clean fuels to be becoming more and more strict. As an important measure to remove the hazardous sulfide from the diesel oil and to produce high quality transportation fuels, hydrotreating process was endowed with great responsibilities to produce ultra clean diesel. The key point of this technology is the design and development of hydrofining catalyst with good physicochemical properties and high activities, especially the synthesis of new composite materials is paid more and more attention to obtain special characteristics in improving its catalytic performance [1–3].

Zeolite beta is a typical representative of porous zeolites with a three-dimensional interconnected channel system of 12-O ring large-pore structure with pore diameters of 0.71 nm × 0.73 nm [4–6], and it also has a tunable and suitable acidity, higher hydroisomerization activity, lower hydrogen-transfer capacity and lower catalyst deactivation ability. Due to its unique pore structure and catalytic properties, beta zeolite is a prospective candidate of catalyst components for wide application in the industrial processes of hydrocracking, hydroisomerization, alkylation and other petrochemical reactions [7], since the presence of acidic sites favors for the bond cleavage.

Zeolite beta can be synthesized in a wide range of silica to alumina ratios from 5 to 200 in the presence of the tetraethylammonium (TEA) cation as structure-directing agent (SDA) under the alkaline conditions with the conventional sources of aluminium and silicon [8–10]. For hydrotreating process, the suitable amounts of intermediate and weak acid sites would be favorable for the hydrodesulfurization (HDS) reactions of refractory sulfur compounds [11,12], while the large amounts of strong acid also improve the secondary reactions involving cracking and coking [13]. Therefore, the controls of SiO_2/Al_2O_3 ratio and beta content in the catalyst will be very important to make a balance between the acidity and hydrodesulfurization activity.

The conventional synthesis method of zeolite beta is hydrothermal crystallization method under relative mild conditions, and others involve vapour-phase transport method, steam-assisted crystallization method, etc. [14,15,7]. In this work, a micro/mesoporous zeolite beta was synthesized by in situ hydrothermal crystallization method using kaolin clay, an abun-

* Corresponding author. Tel.: +86 10 89731586; fax: +86 10 69724721.
E-mail addresses: duanaijun@cup.edu.cn (A. Duan), zhenzhao@cup.edu.cn (Z. Zhao).

0920-5861/$ – see front matter © 2011 Elsevier B.V. All rights reserved.
doi:10.1016/j.cattod.2011.03.044

dant and cheap resource of silicon substrate in the world, as the unique sources of silica and alumina, and the affecting factors of the preparation process, i.e., the ratios of H_2O/SiO_2, the optimal temperature and crystallization time were systematically studied. Furthermore, the composite supports of γ-Al_2O_3 with suitable contents of beta zeolites were prepared by the mechanical mixing method. Then through an incipient-wetness impregnation method, a series of NiMo/Beta-Al_2O_3 supported catalysts were prepared and used in the HDS process of FCC diesel feedstock to investigate their catalytic performances. Based on the characterization results by various techniques the relative interrelations between their characteristics and activities were analyzed and deduced.

2. Experimental

2.1. Beta zeolite preparation

A kind of kaolin clay derived from Suzhou was used to be the unique silica and alumina sources in the work. It needs to be calcined at 720 °C for 5 h to obtain metakaolin at first, then different kinds of acids, i.e., H_2SO_4, HCl and H_3PO_4 solutions, were used to pretreat the metakaolin materials at various conditions to partially remove the hydroxyl group and aluminium ions, which was called acid-treated process. In this process, by controlling the acid leaching degree, the acid concentration and the preparation conditions were adjusted and optimized aiming at obtaining a suitable ratio of SiO_2/Al_2O_3 (~100) and the highest crystallinity. Then, a mixture solution of TEAOH and NaOH was used to treat the above metakaolin, and the formative mixtures were with different molar ratios of Na_2O:Al_2O_3:SiO_2:TEAOH:H_2O. A typical preparation procedure was described in our previous work [16]. Then these composite solutions with different ratios of constituent components were put into a high-pressure oven to proceed to the crystallization of crude materials to zeolite beta products under different temperatures and various times. The operation conditions of the synthesis process were also modified and optimized to obtain high crystallinity. The final solid products of zeolite beta at different preparation conditions were filtered, washed, dried at 120 °C for 6 h and calcined at 550 °C for 6 h.

2.2. Preparations of composite supports and supported catalysts

The above beta zeolites were used as a component of support material combined with Al_2O_3 by mechanical mixing method to obtain a series of composite supports with different contents of zeolite beta. The typical content of beta in the Beta-Al_2O_3 composites are 8 m%, 16 m%, 24 m%, 32 m%, and 40 m%.

The corresponding NiMo catalysts were prepared by using two-step incipient-wetness impregnation method with aqueous solutions of nickle nitrate [$Ni(NO_3)_2{\cdot}6H_2O$] and ammonium heptamolybdate[$(NH_4)_6Mo_7O_{24}{\cdot}4H_2O$] to impregnate the above series composite supports sequentially, of which the metal loadings were kept constantly at 10 m% of MoO_3 and 3.5 m% of NiO. The molybdenum was firstly loaded, and the nickel was introduced in the second time impregnation. After each impregnation steps, the obtained intermediate precursors needed to be insonated in an ultra sonic treater for 30 min to expedite the dispersions of active metal components on the support surface. The prepared samples were dried at 120 °C for 6 h and calcined at 500 °C for 6 h.

2.3. Catalyst characterization method

The total specific surface area, total and micropore volumes, porosity and pore size distribution of the samples were determined by the nitrogen adsorption/desorption method on a Micromeritics ASAP 2020 automated gas adsorption system. Prior to N_2 adsorption, the tested samples were degassed in vacuum at 350 °C. The specific surface areas were determined by the Brunauer–Emmett–Teller (BET) method.

The carriers and the catalysts were characterized using powder X-ray diffraction (PXRD) for phase identification and for crystallite size estimation. PXRD results were obtained from the XRD-6000 diffractometer and the typical conditions of analysis were as follows: voltage 40 kV, 30 mA; scan range from 5° to 80°; step size 4° min^{-1}; type of scan-medium radiation (Cu Kα).

Microscopic observations of samples were examined using a Cambridge S-360 SEM, with which the electron beam strikes the surface at an angle, causing the emission of secondary electrons from the surface atoms and strike a detector to receive and record the signal. Scanning electron microscopy gives information about the surface structure of the sample.

The morphology and microstructure of the samples were characterized by high resolution transmission electron microscopy (HRTEM) on a Philips Tecnai G2 F20 transmission electron microscope operated at an accelerating voltage of 200 kV.

Table 1
The typical properties of diesel feed stock.

Properties	Data
Density (20 °C), g cm^{-3}	0.8613
S, μg/g	1296
N, μg/g	620
Distillation, °C	
IBP	165 °C
30%	246 °C
50%	273 °C
70%	298 °C
FBP	368 °C

2.4. Activity measurement

Catalytic hydrodesulfurization activities of the catalysts were performed in a high-pressure microreactor with 2 g catalyst of 0.3–0.5 mm grain size. The catalysts were presulfided with a solution of 2 m% CS_2–cyclohexane mixture under the conditions of 320 °C, 4.0 MPa, 1.0 h^{-1} and 600 mL mL^{-1} for 6 h. Then, the hydrodesulfurization activities with diesel feed were tested under the conditions of 350 °C, 5.0 MPa, 600 mL mL^{-1} and 1.0 h^{-1} after continuous reaction for 13 h on-stream. The typical properties of diesel feed are shown in Table 1, and S content was as high as 1296 μg g^{-1}.

A LC-4 coulometric sulfur analyzer was used to analyze the sulfur content in the feedstock and the hydrogenated products for comparing the sulfur removal. The samples, in the presence of the accelerator and added oxygen, combusted in the quartz tube to form SO_2 in equilibrium with SO_3. Then the sulfuric mixture was transported by the nitrogen carrier gas into the following furnace at 825 °C and was reduced by copper to convert all SO_3 to SO_2 quantitatively, which was subsequently conveyed to the coulometric cell of the detector. The resulting sulfur dioxide and/or hydrogen sulfide was automatically measured by using coulometric iodometric titration method. The detailed distributions of different sulfides in the feedstock and products were determined by a GC-3420 chromatograph coupled with a HP-5MS column (30 m × 0.25 mm × 0.25 μm) and an OI Analytical Model 5380 pulsed flame photometric detector (PFPD)(America, OI Analytical corporation). The GC oven was maintained at 50°C for 3 min and increased to 300°C at 10°C/min, and then kept at 300 °C for 20 min. The sample injector was working at 300 °C and the PFPD detector was at 250°C.

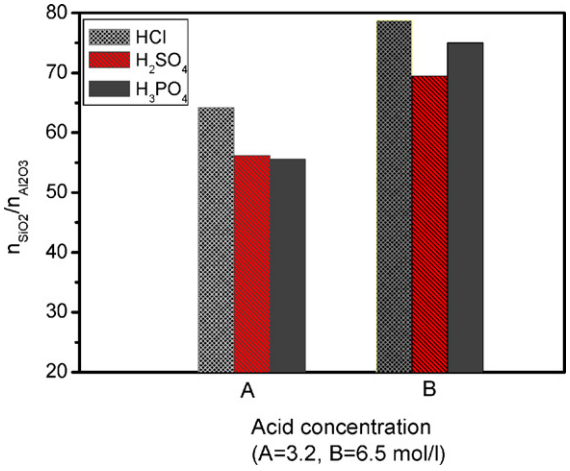

Fig. 1. The effects of acid types on the SiO_2/Al_2O_3 ratio of acid-treated metakaolin.

3. Results and discussion

3.1. Effects of acid-leached conditions

3.1.1. Effects of acid type

Kaolin clay is a kind of finely ground clay mainly produced from minerals in the kaolinite group. It is widely used in paper, coatings, paints, pigments, etc., especially in the production of catalyst carriers in recent year, due to its low price and abundant reserves in the world. As the unique source of silica and alumina, the kaolin clay needs to be pretreated before the formation of zeolite materials. In this research, Suzhou Kaolin clay was calcined firstly and pretreated with different kinds and concentrations of acid solutions, i.e., H_2SO_4, HCl and H_3PO_4 at 90 °C for 3 h in order to partially remove the hydroxyl group and aluminium ions. The resulted clays were so-called acid-treated metakaolins, and their SiO_2/Al_2O_3 ratios were examined by GB/T 14564-1993 analysis method [17]. The typical properties of the above products are shown in Fig. 1.

According to the SiO_2/Al_2O_3 ratios exhibited in Fig. 1, it can be concluded that HCl pretreatment resulted in higher SiO_2/Al_2O_3 ratios than other kinds of acids.

3.1.2. Effects of acid concentration

Using HCl as the acid resource to treat the metakaolin, the effects of acid concentration on SiO_2/Al_2O_3 ratio were investigated in the range of 3–12 mol/L, and the results are shown in Fig. 2. The suitable concentration of HCl is 8.2 mol/L and the highest SiO_2/Al_2O_3 ratio reaches 93.3.

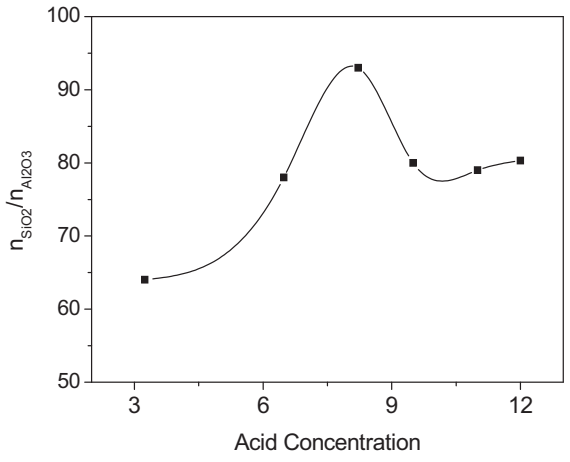

Fig. 2. The effect of acid concentration on the SiO_2/Al_2O_3 ratio of acid-treated metakaolin.

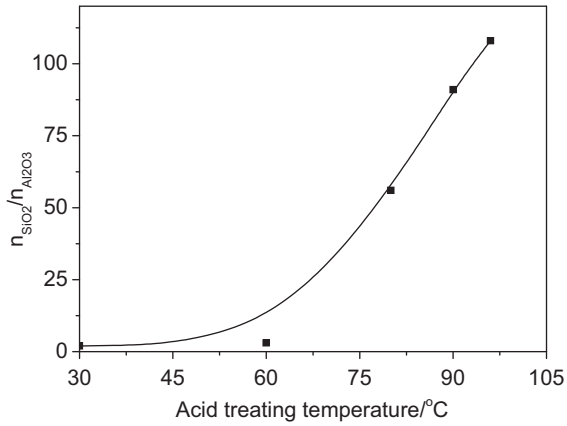

Fig. 3. The effect of temperature on the SiO_2/Al_2O_3 ratio of acid-treated metakaolin.

3.1.3. Effects of temperature in acid treatment

Fig. 3 gives the effects of pretreating temperature on the SiO_2/Al_2O_3 ratio (with HCl of 8.2 mol/L). Along with the increase of the processing temperature to pretreat the metakaolin, the SiO_2/Al_2O_3 ratio goes up sharply since high temperature favors the removal of aluminium ion from the raw material. The result in Fig. 3 demonstrates that high temperature is favorable for getting high SiO_2/Al_2O_3 ratio of acid-treated metakaolin clay. At 96 °C, the SiO_2/Al_2O_3 ratio of β zeolite was ~100, and the β zeolite obtained by aging at 96 °C possesses moderate acidity for HDS.

When the temperature is too high, the dealuminization degree is also high, which is unfavorable to get high crystallinity of Beta and results in weaker acidity of beta zeolite. Thus, the optimal processing temperature is 96 °C and the highest SiO_2/Al_2O_3 ratio reaches 111.5.

3.1.4. Effects of acid treating time

Fig. 4 gives the effects of acid treating time on the SiO_2/Al_2O_3 ratio (with HCl of 8.2 mol/L, at 96 °C). The results indicated that the acid treating time kept for 3 h produces a metakaolin with SiO_2/Al_2O_3 ratio around 100, which may have moderate acidity and is suitable for HDS reactions [11,12].

Based on the above analysis, the conditions of acid treatment should be controlled to obtain the metakaolin with a suitable SiO_2/Al_2O_3 ratio. Thus, the optimal conditions to obtain metakaolin

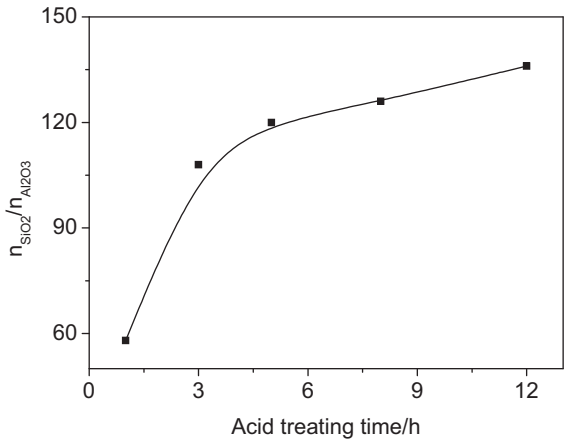

Fig. 4. The effect of treating time on the SiO_2/Al_2O_3 ratio of acid-treated metakaolin.

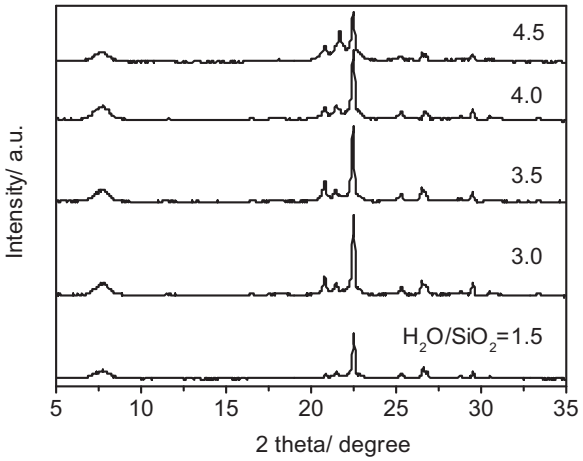

Fig. 5. XRD patterns of zeolite β synthesized at different H_2O/SiO_2 ratios.

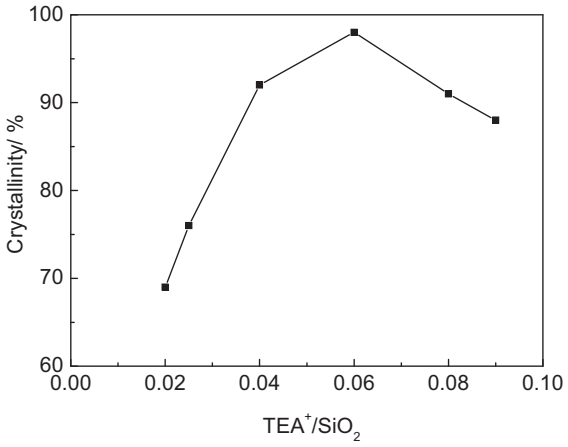

Fig. 6. Crystallinity of zeolite β synthesized at different $TEAOH/SiO_2$ ratios.

material with SiO_2/Al_2O_3 ratio of ~100 are 8.2 mol/L HCl as the acid resource and treating at 96 °C for 3 h.

3.2. Effects of crystallization conditions

Based on the above mentioned method [16], the mixture solutions containing of acid-treated metakaolin, TEAOH, NaOH and deionized water with different molar ratios of $Na_2O:Al_2O_3:SiO_2:TEAOH:H_2O$ were used as the synthesis reagents for obtaining zeolite beta. Then the crystallization process and aftertreatment procedure were executed to obtain zeolite beta samples. The synthesis conditions were investigated to achieve higher crystallinity and good properties.

3.2.1. Effects of H_2O/SiO_2 ratios

Fig. 5 shows the XRD analysis results of different beta samples synthesized with different initial H_2O/SiO_2 ratios. XRD patterns shows that the peaks at 2θ of 7.7, 21.4 and 22.5° are ascribed to the characteristics of zeolite beta and the shoulder peaks at 21–22° are belonged to the different polymorphs A, B and C of zeolite beta [18]. The H_2O/SiO_2 ratio in the synthesis mixture has a great influence on the crystallinity of zeolite beta based on the intensity of peak at 22.5° which is typical of the Beta topology. When the ratio of H_2O/SiO_2 is 3.0, the maximal relative crystallinity of the as-synthesized samples is 98.3 and this sample has a high surface area (574 m^2/g) and pore volume (0.38 cm^3/g). This is attributed to the good solubility of alumina and silica species in the kaolin clay, and the suitable hydrolysis and nucleation rate under the condition of relatively low water content in the synthesis solution. For the sample prepared with a higher water content (such as $H_2O/SiO_2 = 4.5$), a lower intensity of XRD peak at 22.5° is observed, which is attributed to that the high H_2O/SiO_2 ratio decreases the alkalinity of system and dilutes the concentrations of primary species of aluminium and silica, presumably leads to slower nucleation and crystallization rates, consequently lowers crystallinity of the beta sample [19,20]. So the suitable ratio of H_2O/SiO_2 is 3–4 in the synthesis of the zeolite beta from kaolin clay.

3.2.2. Effects of TEAOH

TEA^+ is usually used as the structure directing agent to compose zeolite beta. Combined with the effects of OH^- and H_2O, TEA^+ construct the configurations of silica to form the zeolite beta framework. The effect of TEAOH solution addition on the relative crystallinity of beta was investigated in this work. As shown in Fig. 6, the $TEAOH/SiO_2$ ratio of 0.06 is confirmed to be the optimum value based on the relative crystallinities of the investigated samples. As the concentration of TEAOH is too low, it will be hard for moderate TEA^+ ions to act as template for the formation of beta framework. Excessive addition of TEAOH into the synthesis mixture, on the one hand, accelerates the dissolution rate of the acid-treated metakaolin to produce aluminium and silica species, which facilitates the beta formation [21]. On the other hand, it also results in the increase of the alkaline degree of the synthesis system which promotes the autolysis of the Beta nanocrystal generated initially, then these contradictory influences lead to a lower beta crystallinity [22].

3.2.3. Effects of alkaline

Zeolite beta was typically synthesized under alkaline condition [23]. Alkalinity control is very significant to the constructruction of beta zeolite framework. Na_2O/SiO_2 ratio represents the alkalinity of the synthesis system in the crystallization process. Fig. 7 shows the relative crystallinity tendency of zeolite beta derived from different Na_2O/SiO_2 ratios. The results show that the relative crystallinity of beta zeolites increases with the increasing Na_2O/SiO_2 ratio at first and reaches the maximum at the Na_2O/SiO_2 ratio of 0.05. The possible explanation might be related to the facile dissolution of the acid-treated metakaolin. Nevertheless, with the further increase of Na_2O/SiO_2 ratio, the strong alkalinity promotes the autolysis of the zeolite beta produced incipiently and results in the decrease of the relative crystallinity of beta zeolite samples.

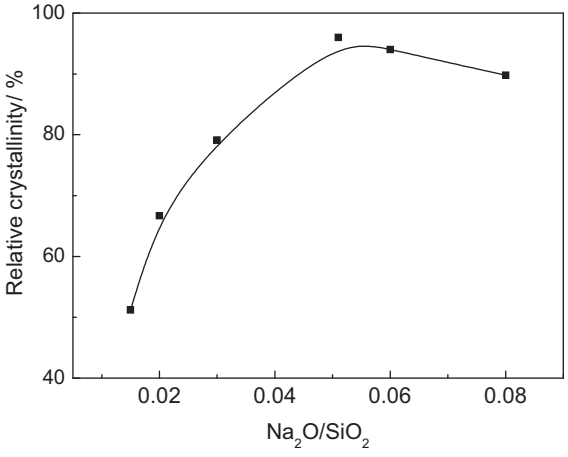

Fig. 7. Crystallinity of zeolite β synthesized at different Na_2O/SiO_2 ratios.

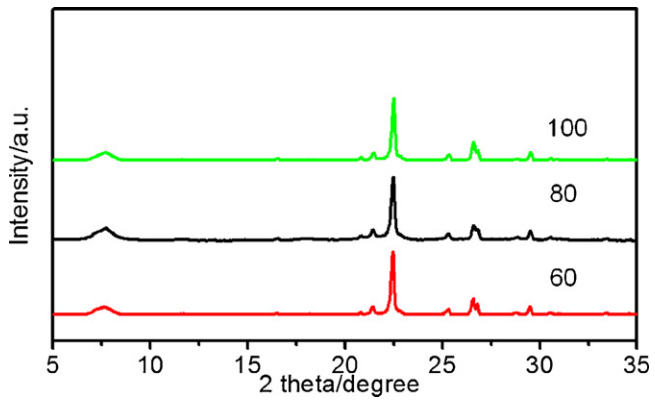

Fig. 8. XRD patterns of zeolite β synthesized at different SiO_2/Al_2O_3 ratios (60, 80 and 100).

3.2.4. *Effects of SiO_2/Al_2O_3 ratios*

In order to obtain different materials with different acidities and textural properties [22,24], various SiO_2/Al_2O_3 ratios of the raw materials in the synthesis system were adopted in this research. Fig. 8 gives the XRD patterns of zeolite β obtained from different SiO_2/Al_2O_3 ratios in initial feed, and the diffraction peak at 22.5° was assigned to d302 of beta zeolites with different SiO_2/Al_2O_3 ratios. The crystallinities of different samples with the SiO_2/Al_2O_3 ratios of 60, 80 and 100 are 96.7, 98.3 and 98.1, respectively, indicating that zeolite beta products with different SiO_2/Al_2O_3 ratios can be well synthesized under the investigated conditions and the degrees of crystallization are relatively impeccable.

3.2.5. *Effects of crystallization temperature*

The effect of crystallization temperature on the crystallinity of beta zeolite was studied in the range of 140–190 °C. The variable tendency of relative crystallinity is given in Fig. 9 and the FT-IR spectra of zeolite β products obtained at different reaction temperatures are shown in Fig. 10.

The crystallinity data in Fig. 9 demonstrates that the beta zeolite developed well under the crystallization temperature from 140 to 190 °C, and the crystallinity reached as high as 100 as the crystallization temperature was kept at 170 °C.

According to the analysis results of Mozgawa [25], the absorbtion bands in 500–800 cm^{-1} region can be assigned to the external vibrational modes of the tetrahedron rings and the absorption bands belonged to the vibration modes of single 6-membered rings (S6R) and double 4-membered rings (D4R) sit at ~670 and

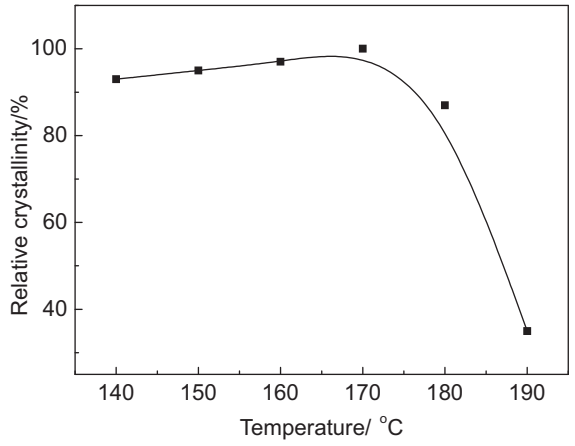

Fig. 9. Crystallinity of zeolite β synthesized at different crystallization temperatures.

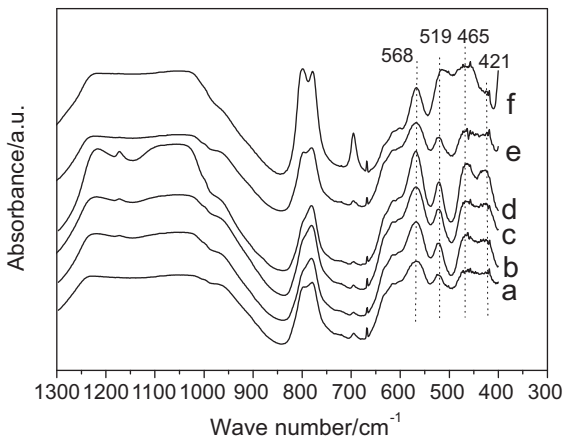

Fig. 10. FT-IR spectra of the zeolite β products synthesized at different reaction temperatures: (a) 140 °C; (b) 150 °C; (c) 160 °C; (d) 170 °C; (e) 180 °C; (f) 190 °C.

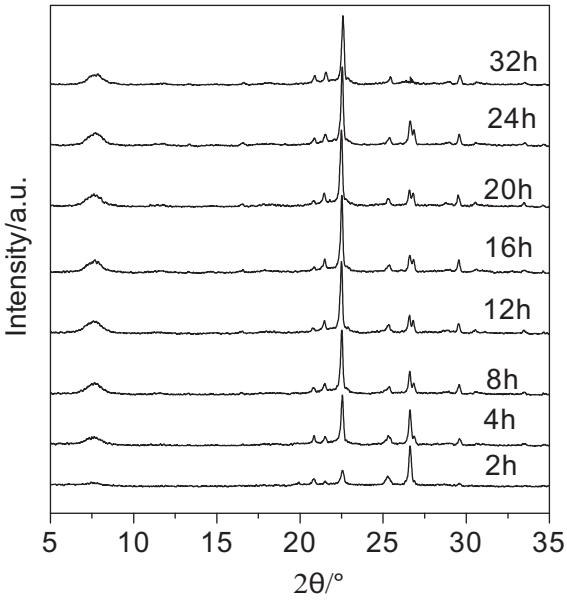

Fig. 11. XRD spectra of zeolite beta synthesized with various crystallization times.

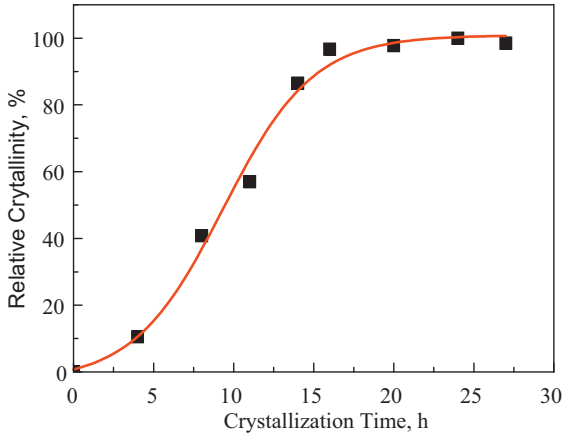

Fig. 12. Crystallinity of zeolite β synthesized with different crystallization times.

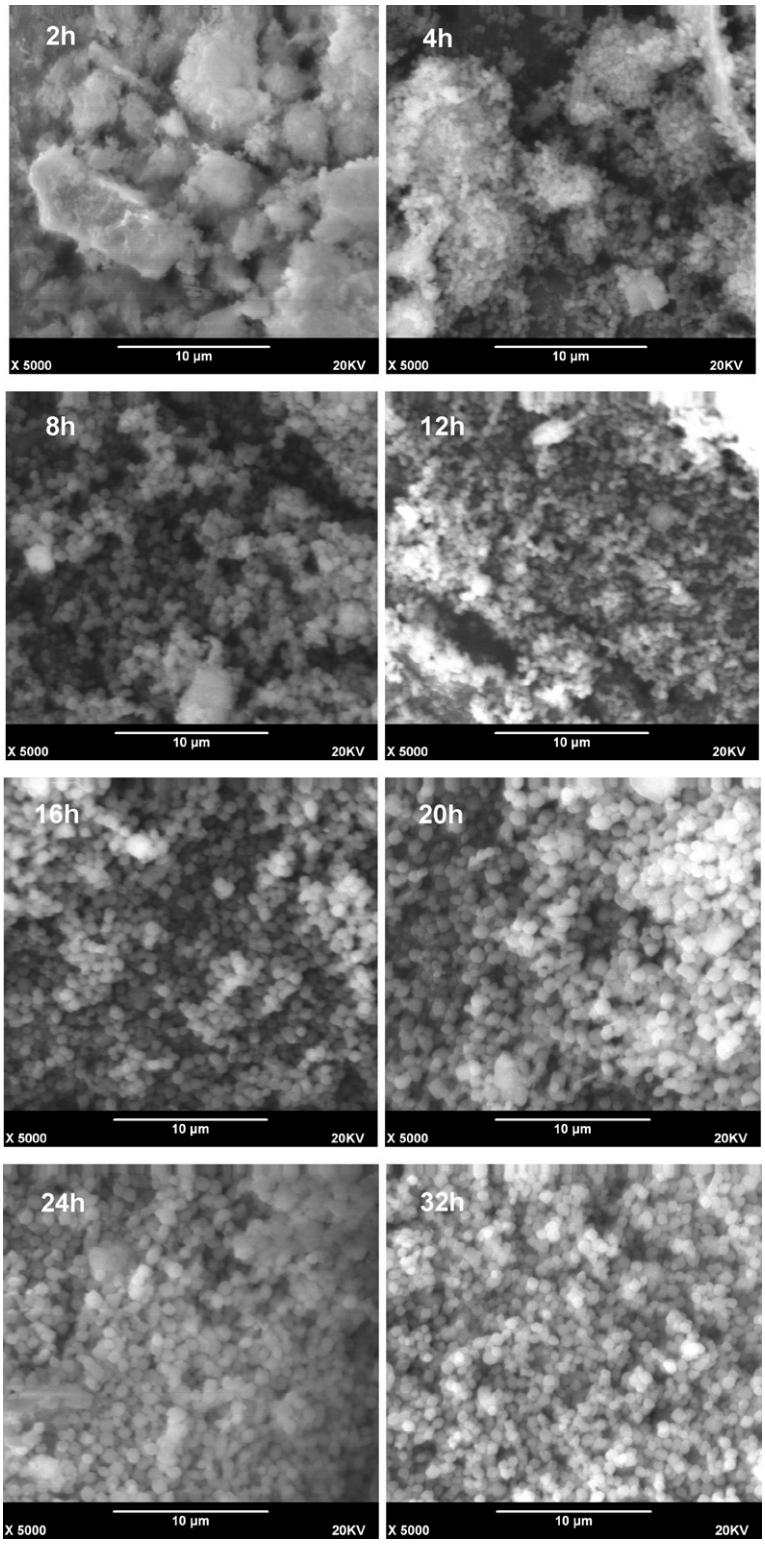

Fig. 13. SEM images of the β zeolite products synthesized with different crystallization times.

~560 cm^{-1}, respectively. Scanu et al. [26] also reported that the absorption bands centred at 930 and 1200 cm^{-1} might be attributed to the intramolecular vibrations of AlO_4 and SiO_4 tetrahedra, and the absorption bands in 400–500 cm^{-1} region were derived from the bending modes of the Si–O–Al bonds. From the FT-IR spectra in Fig. 10, the typical peaks at 421 cm^{-1} and 465 cm^{-1} are ascribed to corresponding internal bending modes of the Si–O–Al bonds, and bands at 519 cm^{-1} and 568 cm^{-1} are attributed to the D4R vibration. The band at around 700 cm^{-1} maybe assigned to the vibration of Al_2O_3 [27] or the interbonding vibration of O–Si(Al)–O [28]. From the curve of 190 °C in Fig. 10, the intensity of 700 cm^{-1} becomes more intense, which might be assigned to the separated phases of Al_2O_3 or SiO_2 formed at high crystallization temperature of 190 °C due to the rapid self-seeding nucleation. Furthermore, the intensities of the main peaks centered at 400–650 cm^{-1} are relatively strong in the spectra of the samples obtained at 150–170 °C, espe-

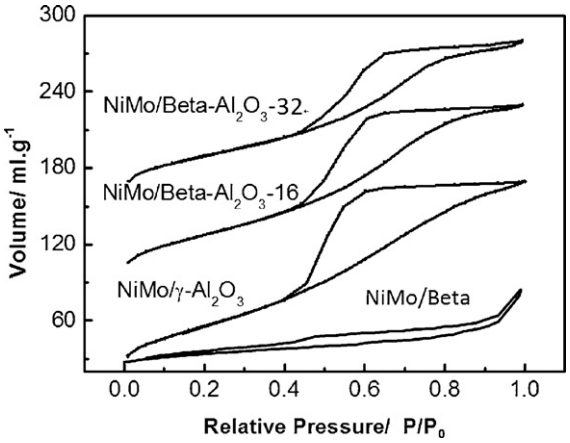

Fig. 14. The nitrogen adsorption/desorption isotherms of NiMo/Beta-Al_2O_3 catalysts.

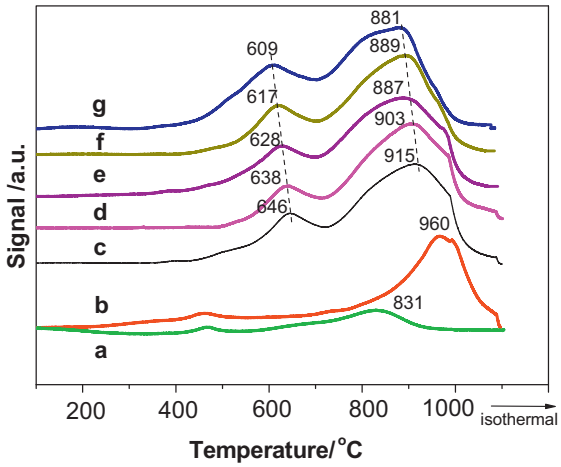

Fig. 15. H2-TPR profiles of the NiMo supported catalysts. (a) Ni/Al_2O_3; (b) Mo/Al_2O_3; (c) $NiMo/Al_2O_3$; (d)$NiMo/Beta-Al_2O_3$-8; (e) $NiMo/Beta-Al_2O_3$-16; (f) $NiMo/Beta-Al_2O_3$-32; (g) $NiMo/Beta-Al_2O_3$-40.

cially at 170 °C, indicating that the crystallization of zeolite grows well at the crystallization temperature of 170 °C.

3.2.6. *Effects of crystallization time*

XRD patterns in Fig. 11 indicate that there is nanocrystal beta formed at 2 h and the peak intensities increase sharply after crystallization for 4 h. From the crystallization curve in Fig. 12, which exhibits a typical S-shaped trend, it can be deduced that the induction period is very short and less than 5 h, and after 16 h the crystallinity becomes stable. From the SEM images of beta zeolite samples obtained at different crystallization times in Fig. 13, it is also known that the crystallinities and particle sizes increase with the crystallization time, and the samples obtained after crystallization for 16 h exhibit well facetted crystal morphologies and unique crystal size.

Based on the above discussion, the optimal conditions for the beta zeolite synthesis are H_2O/SiO_2 of 3–4, $TEAOH/SiO_2$ ratio of 0.06, Na_2O/SiO_2 ratio of 0.05, crystallization temperature of 170 °C and more than 16 h for crystallization time.

3.3. *Typical physico-chemical properties of the synthesized samples*

Under the optimal conditions for the synthesis of zeolite beta, a kind of sample with the SiO_2/Al_2O_3 ratio of ~100, with which the material has an appropriate acid property for HDS reaction, was synthesized and a series of composite support of Beta-Al_2O_3 with different beta contents of 8, 16, 24, 32 and 40 were prepared by a mechanical mixing method. The corresponding supported NiMo catalysts were prepared by the series impregnation methods to investigate their HDS performance with diesel feedstock.

Table 2 lists the typical physico-chemical properties of zeolite beta, the support and the relative catalysts. The obtained beta zeolite has a higher surface area of 573.5 m^2/g, and the average pore diameter is 3.71 nm. The relative carriers of $Beta/Al_2O_3$-16 and $Beta/Al_2O_3$-32, the suffix number represents the percentages of beta zeolites in the support compositions, also show higher surface areas compared with the traditional carrier of Al_2O_3. However, from Fig. 14, the N_2 adsorption–desorption curves of different samples reveal type IV isotherms, which are the characteristics of mesoporous materials. Compared with that of NiMo/Beta catalyst, the others have more mesopores. The co-existences of micro- and mesoporous structures of the composite carriers may facilitate the diffusion process of reactant molecules to access the internal metallic active sites on the surface of catalyst and result in high hydrotreating activity.

Fig. 15 shows the H_2-TPR profiles of the supported NiMo catalysts. H_2-TPR experiment can reflect the reductibility of the active species on the catalysts. And the reductibility is closely related to the interaction between the active metal species and the support. So different interactions between surface active species and support may result in different H_2-TPR patterns. In Fig. 15, there are two typical reduction peaks in the ranges of 500–700 °C and 700–1000 °C. And the peak at high temperature can be ascribed to the reduction of tetrahedral molybdate species and nickel species and the peak at low temperature can be attributed to the reduction of octahedral molybdate species [29,30]. Furthermore, the series catalysts containing beta zeolite show an easily reduced tendency i.e., shifting toward lower temperatures by comparing the peak positions of conventional Ni/Al_2O_3, Mo/Al_2O_3 and $NiMo/Al_2O_3$ catalysts, implying that the introduction of beta zeolite to the support could adjust the interaction between the support and the active metal species and result in the formation of octahedral molybdate species which are the precursors of active phases in HDS catalysts [31–34].

3.4. *HDS performances of beta-incorporated catalysts*

Table 3 exhibits the HDS activity results over different catalysts. The $NiMo/Beta-Al_2O_3$ catalysts exhibit higher HDS efficiencies compared with the conventional $NiMo/Al_2O_3$ catalysts, and they can produce high-quality and low-sulfur diesel from sulfurous feedstock. The S contents in products are lowered to 15 $\mu g\,g^{-1}$ as the zeolite contents are of 24–40 m% in the support, and the best product with S of 8.4 $\mu g\,g^{-1}$ which meets the S regulation of ultra clean diesel in Euro-V specification. The suitable amount of beta addition in the support is 32% since high contents of zeolite beta in the catalyst will accelerate the unwanted side reactions of catalytic cracking and coking, finally result in the catalyst deactivation.

Table 4 shows the detailed distribution of sulfur compounds in feed and in products over $NiMo/Al_2O_3$ and $NiMo/Beta-Al_2O_3$ catalysts. The sulfur distributions of products obtained from the $NiMo/Beta-Al_2O_3$ series catalysts indicate that the addition of beta into the supports improves the depth of sulfur removal, especially enhances the hydrogenation of the refractory sulfur compounds of alkyl-DBT. The acidic catalyst could provide more acid sites for the chemical bond cleavage in HDS reaction, and favor the alkyl group transfer to alleviate the effects of steric hindrance [35–38], which will result in enhancing the deep hydrodesulfurization efficiency.

Table 2
Typical physicochemical properties of different materials.

Samples	S_{BET}/$m^2\ g^{-1}$	Micropore surface area/$m^2\ g^{-1}$	V_{BJH}/$cm^3\ g^{-1}$	Micropore volume/$cm^3\ g^{-1}$	Average pore diameter/nm
Kaolin	28.5	0.0	0.30	0.05	3.77
Beta	573.8	452.3	0.38	0.25	3.71
Al_2O_3	203.0	92.6	0.31	0.14	5.41
Beta/Al_2O_3-16	236.8	212.1	0.29	0.18	4.45
Beta/Al_2O_3-32	271.4	237.6	0.29	0.22	3.93
NiMo/Beta-Al_2O_3-16	186.50	143.2	0.24	0.14	3.89
NiMo/Beta-Al_2O_3-32	164.83	137.7	0.25	0.20	3.72

Table 3
HDS results of FCC diesel over supported NiMo catalysts with various supports.

Catalysts	Sulfur contents in feed ($\mu g\ g^{-1}$)	Sulfur contents in product ($\mu g\ g^{-1}$)	HDS efficiency %
NiMo/Al_2O_3	1296	33.3	97.4%
NiMo/Beta-Al_2O_3-8	1296	32.4	97.5%
NiMo/Beta-Al_2O_3-16	1296	20.6	98.4%
NiMo/Beta-Al_2O_3-24	1296	15.1	98.8%
NiMo/Beta-Al_2O_3-32	1296	8.4	99.4%
NiMo/Beta-Al_2O_3-40	1296	12.8	99.0%

Table 4
The sulfur compounds in feed and in products after HDS over NiMo/Al_2O_3 and NiMo/Beta-Al_2O_3 catalysts.

Sulfur compound	Feed/$\mu g\ g^{-1}$	NiMo/Al_2O_3/$\mu g\ g^{-1}$	NiMo/Beta-Al_2O_3-16/$\mu g\ g^{-1}$	NiMo/Beta-Al_2O_3-32/$\mu g\ g^{-1}$	NiMo/Beta-Al_2O_3-40/$\mu g\ g^{-1}$
BT	25.7	–	–	–	
C1-BT	138.9	–	–	–	
C2-BT	254.8	–	–	–	
≥C3-BT	336.7	–	–	–	
DBT	49.5	–	–	–	
C1-DBT	141.6	–	–	–	
C2-DBT	143.7	14.4	11.2	5.2	6.8
≥C3-DBT	205.1	18.9	9.4	3.2	6.6
Total	1296.0	33.3	20.6	8.4	12.8

Notes: BT – benzothiophene; DBT – dibenzothiophene; C1, C2 and C3 – the numbers of carbon atoms in substituents connected with the BT or DBT rings are 1, 2 and 3 respectively.

In this work, we focus on the systematical study on the synthesis process of Beta from Kaolin raw material. The catalysts prepared in this work contained NiMo bimetallic active species (10 m% of MoO_3 and 3.5 m% of NiO) and with optimal SiO_2/Al_2O_3 ratio around 100. However, in our previous work the prepared catalysts were with NiW bimetallic active species (27 m% of WO_3 and 3.5 m% of NiO) and with SiO_2/Al_2O_3 ratio of 88. Compared the HDS results in this work with those in our previous works [16], the HDS efficacy of NiMo/Beta-Al_2O_3-32 catalyst (99.4%), which has lower loadings of active metals, was greater than that of NiW/Al_2O_3-MB (98.7%), and also exhibited a similar activity to that of NiW/TiO_2–Al_2O_3–MB (99.3%), which was Ti-modified catalyst. Therefore, through the optimization of Beta synthesis, the catalytic property for HDS could also be improved in this study.

Based on the discussion above, it can be concluded that the incorporation of acidic zeolite beta into the support could adjust the acid distributions of catalyst and improve the cleavage of C–S bonds which would facilitate the removal of sulfur in the feedstock, but the further cracking and coke deposition should be controlled by limiting the beta content and choosing the suitable SiO_2/Al_2O_3 ratio for avoiding the undesirable deactivation of catalyst.

4. Summary

(1) Kaolin clay was treated by H_2SO_4, HCl and H_3PO_4 solutions to obtain high crystallinity of metakaolin under different pretreating conditions. The optimal conditions were the HCl concentrations of 8.2 mol/L, the processing temperature of 96 °C and the treating time of 3 h for obtaining a metakaolin with SiO_2/Al_2O_3 ratio of ~100.

(2) Zeolite beta was synthesized by in situ hydrothermal crystallization method from the raw material of acid-treated metakaolin. Through the optimization and the modulation of crystallization parameters of H_2O/SiO_2 ratios, TEAOH/SiO_2 ratio, Na_2O/SiO_2 ratios, the crystallization temperature and time, zeolite beta with high crytallinity and micro/mesoporous structure was obtained under the conditions of H_2O/SiO_2 of 3–4, TEAOH/SiO_2 ratio of 0.06, Na_2O/SiO_2 ratio of 0.05, crystallization temperature of 170 °C and more than 16 h for crystallization time.

(3) The catalytic HDS performances indicated that NiMo/Beta-Al_2O_3 catalysts exhibited higher HDS activities compared with the conventional NiMo/Al_2O_3 catalysts, and also produce high-quality diesel products with S contents lower than 15 $\mu g\ g^{-1}$. And the suitable amount of beta added in the support was 32% for getting the highest HDS efficiency over NiMo/Beta-Al_2O_3 catalyst, of which the sulfur content met the S regulation of ultra clean diesel fuel in Euro-V specification.

(4) The incorporation of acidic zeolite into the support could provide more acid sites for HDS and favored the deep removal of sulfur compounds. However, the beta contents should be controlled for avoiding the undesirable side reactions of cracking and coking.

Acknowledgements

The authors acknowledge the financial supports from NSFC (Nos. 20876173, 21073235 and 20833011), Ministry of Education key project of China (No. 31) and CNPC-Petrochemical Research Institute project (No. 2008A-3801).

References

[1] L. Ding, Y. Zheng, Z. Zhang, J. Catal. 241 (2006) 435.
[2] Y. Tao, H. Kanoh, K. Kaneko, J. Am. Chem. Soc. 125 (2003) 6044.
[3] A. Bordoloi, B.M. Devassy, P.S. Niphadkar, J. Mol. Catal. A: Chem. 253 (2006) 239.
[4] C. Baerlocher, W.M. Meier, D.H. Olson, Atlas of Zeolite Framework Types, Elsevier, Amsterdam, 2001, p. 77.
[5] J.M. Newsam, M.M.J. Treacy, W.T. Koetsier, C.B. de Gruyter, Proc. R. Soc. Lond., Ser. A 420 (1988) 375.
[6] J.B. Higgins, R.B. Lapierre, J.L. Schlenker, A.C. Rohrman, J.D. Wood, G.T. Kerr, Zeolites 8 (1988) 446.
[7] M. Matsukata, T. Osaki, M. Ogura, Micropor. Mesopor. Mater. 56 (2002) 1.
[8] R.B. Borade, A. Clearfield, Chem. Commun. 5 (1996) 625.
[9] F. Vaudry, F. Di Renzo, P. Espiau, F. Fajula, P. Schulz, Zeolites 19 (1997) 253.
[10] O. Larlus, S. Mintova, S.T. Wilson, R.R. Willis, H. Abrevaya, T. Bein, Micropor. Mesopor. Mater. 269 (2010) 71.
[11] M. Breysse, C.E. Hédoire, C. Louis, G. Pérot, Science and technology in catalysis, 2002, in: M. Anpo, M. Onaka, H. Yamashita (Eds.), Proceedings of the Fourth Tokyo Conference on Advanced Catalytic Science and Technology, Deep Hydrodesulfurization: Reactions and Catalysts, Tokyo, 2002, p. 119.
[12] C. Thomas, L. Vivier, A. Travert, F. Maugé, S. Kasztelan, G. Pérot, J. Catal. 179 (1998) 495.
[13] J. Hagen, Industrial Catalysis: A. Practical Approach, Wiley-VCH, Weinheim, 2006, p. 201.
[14] M.A. Camblor, A. Mifsud, J. Pérez-Pariente, Zeolites 11 (1991) 792.
[15] P.R. Hari Prasad Rao, K. Ueyama, M. Matsukata, Appl. Catal. A: Gen. 166 (1998) 97.
[16] G. Wan, A. Duan, Y. Zhang, Z. Zhao, G. Jiang, D. Zhang, Z. Gao, Catal. Today 149 (2010) 69.
[17] GB/T 14563-2008, Kaolin clay chemical analysis method in China.
[18] M. Bregolato, V. Bolis, C. Busco, P. Ugliengo, S. Bordiga, F. Cavani, N. Ballarini, L. Maselli, S. Passeri, I. Rossetti, L. Forni, J. Catal. 245 (2007) 285–300.
[19] M.D. Kadgaonkar, M.W. Kasture, D.S. Bhange, P.N. Joshi, V. Ramaswamy, R. Kumar, Micropor. Mesopor. Mater. 101 (2007) 108–114.
[20] Sinkó Katalin, Materials 3 (2010) 704.
[21] G. Shao, J. Yang, X. Zhang, G. Zhu, J. Wang, C. Liu, Mater. Lett. 61 (2007) 1443.
[22] T. Selvam, C. Aresipathi, G.T.P. Mabande, H. Toufar, W. Schwieger, J. Mater. Chem. 15 (2005) 2013.
[23] X. Feng, Y. Liu, C. Liu, C. Liu, H. Wang, J. Adv. Mater. Res. 79–82 (2009) 2271.
[24] W. Schmidt, A.V. Toktarev, F. Schüth, K.G. Ione, K. Unger, Stud. Surf. Sci. Catal. 135 (2001) 190.
[25] W. Mozgawa, J. Mol. Struct. 596 (2001) 129.
[26] T. Scanu, J. Guglielmi, P. Colomban, Solid State Ionics 70–71 (1994) 109.
[27] A. Hajimohammadi, J.L. Provis, J.S.J. Deventer van, Ind. Eng. Chem. Res. 47 (23) (2008) 9396.
[28] Y. Li, X. Wang, Y.C. Dong, J.W. Zhu, Trans. Nonferrous Met. Soc. China 12 (2) (2002) 321.
[29] R. López Cordero, F.J. Gil Llambias, A. López Agudo, Appl. Catal. 74 (1991) 125.
[30] C.R. Lopez, A. Lopez Agudo, Appl. Catal. A: Gen. 202 (2000) 23.
[31] H. Topsøe, B.S. Clausen, F.E. Massoth, in: J.R. Anderson, M. Boudart (Eds.), Hydrotreating Catalysts Catalysis Science and Technology, vol. 11, Springer, Berlin, 1996.
[32] Z.H. Luan, L. Kevan, Micropor. Mesopor. Mater. 44 (2001) 337.
[33] V.H.J. DeBeer, J.C. Duchet, R. Prins, J. Catal. 72 (1981) 369.
[34] J.C. Duchet, E.M. Van Oers, V.H.J. DeBeer, R. Prins, J. Catal. 80 (1983) 386.
[35] E. Lecrenay, K. Sakanishi, I. Mochida, Appl. Catal. A: Gen. 175 (1998) 237.
[36] M.V. Landau, D. Berger, M. Herskowitz, J. Catal. 159 (1996) 236.
[37] P. Michaud, J.L. Lemberton, G. Pérot, Appl. Catal. A: Gen. 169 (1998) 343.
[38] X. Rozanska, X. Saintigny, R.A. Santen van, J. Catal. 208 (2002) 89.